Chế tạo màng cellulose acetate hoạt tính chứa tinh dầu oregano và sodium alginate dùng trong bao bì thực phẩm

Đặng Thị Tố Nữ*, Nguyễn Thụy Ngọc Trâm, Võ Thị Trọng Hoa

Khoa Khoa học Tự nhiên, Trường Đại học Quy Nhơn, Việt Nam

TÓM TẮT

Nghiên cứu này phát triển và đánh giá các màng cellulose acetate (CA) kết hợp với tinh dầu oregano (OEO) và sodium alginate (SA) nhằm ứng dụng làm bao bì thực phẩm hoạt tính. OEO là một chiết xuất thực vật tự nhiên có đặc tính kháng khuẩn và chống oxy hóa, được nhũ hóa bằng cách kết hợp pha dầu và pha nước để tạo thành hỗn hợp ổn định sau đó nhỏ từng giọt có kiểm soát vào gel CA trước khi tạo màng. Các màng được tạo ra bằng phương pháp đúc và được khảo sát hoạt tính chống oxy hóa, khả năng kháng khuẩn, đặc tính cản hơi nước, phổ IR, phân tích nhiệt và hình thái bề mặt. Hoạt tính chống oxy hóa được định lượng bằng phương pháp DPPH (2,2-diphenyl-1-picrylhydrazyl), cho thấy khả năng bắt gốc tự do tăng theo nồng độ, với màng CA/SA/OEO 4.5% đạt hiệu quả 84%. Thử nghiệm kháng khuẩn cho thấy vùng ức chế vi khuẩn là 35 mm đối với *Escherichia coli* và 44 mm đối với *Staphylococcus aureus*. Phân tích bằng kính hiển vi điện tử quét (SEM) cho thấy sự phân bố đồng đều của các giọt nhũ tương giúp cải thiện cấu trúc màng và tăng cường đặc tính cản hơi nước. Những kết quả này cho thấy màng CA chứa tinh dầu oregano là vật liệu phân hủy sinh học đầy hứa hẹn với nhiều chức năng cho ứng dụng bao bì thực phẩm hoạt tính.

Keywords: *CA/SA/OEO, oregano, gel nhũ tương, bao bì hoạt tính.*

*Tác giả liên hệ chính.
Email: dangthitonu@qnu.edu.vn

Preparation of cellulose acetate-based active films containing oregano essential oil and sodium alginate for food packaging

Dang Thi To Nu*, Nguyen Thuy Ngoc Tram, Vo Thi Trong Hoa

Faculty of Natural Sciences, Quy Nhon University, Vietnam

ABSTRACT

This study developed and evaluated cellulose acetate (CA)-based films incorporating oregano essential oil (OEO) and sodium alginate (SA) for application as active food packaging. OEO, a natural plant extract with known antimicrobial and antioxidant properties, was emulsified by combining oil and water phases to form a stable mixture, which was then added dropwise into the CA gel before film formation. Films were produced using the casting method and investigated for antioxidant and antimicrobial activities, water vapor barrier properties, infrared spectra (IR), thermal behavior, and morphological characteristics. Antioxidant activity was quantified using the DPPH (2,2-diphenyl-1-picrylhydrazyl) assay, which demonstrated a concentration-dependent increase in radical scavenging, with the CA/SA/OEO 4.5% film achieving 84% activity. Antimicrobial assays, which test a material's ability to inhibit the growth of bacteria, indicated inhibition zones of 35 mm against *Escherichia coli* and 44 mm against *Staphylococcus aureus*. Scanning electron microscopy (SEM) analysis showed that uniform dispersion of emulsion droplets improved film structure and enhanced barrier properties. These findings indicate that CA-based films containing oregano essential oils are promising biodegradable and multifunctional materials for active food packaging.

Keywords: *CA/SA/OEO, oregano, emulsion gel, active packaging*.

1. INTRODUCTION

In recent years, food safety has gained significant attention, leading to an increased demand for "natural" antibacterial agents. Essential oils (EOs), derived from plant secondary metabolites, have gained attention as safe and effective natural preservatives due to their broad-spectrum antibacterial properties.[1-3] Currently, EOs are utilized in various fields, including food preservation, biomedicine, and cosmetics. Among them, oregano essential oil (Origanum vulgare) has been reported to possess strong antibacterial properties, effectively combating pathogens in fruits and food due to its high concentration of phenolic compounds such as carvacrol and thymol.[1,2,4]

The development of new, effective, biodegradable, and non-toxic materials for fruit and food preservation films has been attracting increasing attention from researchers.[5,6] Cellulose acetate (CA) is one of the environmentally friendly polymers widely used in packaging materials, and thus, many studies have focused on creating active films based on this biopolymer.[7-10] However, CA has some inherent drawbacks such as low flexibility and poor moisture barrier properties, limiting its application in food preservation packaging.

---

*Corresponding author.
Email: dangthitonu@qnu.edu.vn

Sodium alginate (SA) is an anionic polysaccharide with polyhydroxyl and carboxyl groups, typically extracted from brown algae, making it non-toxic and environmentally friendly. SA provides strong gel-forming, emulsifying, and film-forming properties.[11,12] Its capacity to form hydrogel networks and prevent droplet aggregation makes it well-suited as an emulsifier for EO-based emulsions.[13] Additionally, its ability to incorporate antioxidant and antibacterial compounds positions it as a valuable additive for enhancing the properties of food packaging films.[14,15]

Despite the potential of essential oils in packaging, challenges remain in achieving uniform dispersion, maintaining mechanical integrity, and controlling the release of active compounds. The emulsification of OEO has proven to be an effective strategy for enhancing its stability and reducing volatility.[16,17] Choosing the right emulsifier is crucial for making stable OEO emulsions. Previous studies have shown that using emulsification agents such as Tween 80 or SA not only improves the stability of essential oil emulsions but also increases their antimicrobial efficacy against pathogens like *Shewanella putrefaciens* and *Shigella sonnei*, while boosting antioxidant activity.[13,18] However, there have been no studies combining OEO with cellulose acetate films using the emulsification method. This study aims to develop and characterize CA-based films with OEO, SA and Tween 80, focusing on their antioxidant and antimicrobial activities, water vapor barrier properties, and structural features. The findings are intended to advance biodegradable active packaging materials for food preservation.

2. MATERIALS AND METHODS

2.1. Materials

Cellulose acetate (CA, M_w = 30,000 g/mol, containing 39% acetyl groups) was purchased from Sigma-Aldrich (USA). Sodium alginate (analytical reagent grade) and Tween 80 were obtained from Shanghai Zhanyun Chemical Co., Ltd (China). Acetone (99%) was supplied by Xilong (China), and pure oregano essential oil (OEO, 100%) was sourced from KeyPharm (Belgium).

2.2. Films preparation

The emulsion preparation method was carried out based on the report of Baranauskaite with modifications.[17] A 2% sodium alginate (SA) solution was initially prepared by dissolving SA in distilled water, followed by continuous stirring at 60 °C for 3 hours to obtain a homogeneous gel. The stirring process was maintained while gradually cooling the gel to room temperature. Subsequently, Tween-80 and oregano essential oil (OEO) were incorporated into the SA solution under magnetic stirring at a ratio of 0.15:0.4:5 (Tween-80:OEO:SA) for 60 minutes at room temperature, resulting in the formation of the SA/OEO emulsion.

CA/SA/OEO films were prepared using the solvent evaporation casting method. CA (8% w/w) was dissolved in acetone and stirred at 50 °C for 3 hours to form a gel. The emulsion was added dropwise to the CA solution under continuous stirring at room temperature at concentrations of 0%, 3%, 4.5%, and 6% v/v, corresponding to CA/SA/OEO 0%, 3%, 4.5%, and 6%. After 2 hours, a homogeneous emulsion-gel mixture formed. The mixture was left undisturbed for 2 hours to remove air bubbles, then poured onto a glass plate and spread with a casting knife at 250 μm thickness and 1 mm/s speed. Films were left at room temperature for 40 minutes to complete phase inversion, then removed with tweezers and stored in zip-lock bags for analysis.

2.3. Film characterization

2.3.1. Moisture content (MC), total soluble matter (TSM) and water vapor transmission rate (WVTR)

Moisture content (MC) determined by the method of Erceg et al.[10] The films were initially weighed at room temperature as m_1 (g), then dried at 105°C until their mass stabilized, at which point

it was recorded as m_2 (g). The calculation was performed using the following equation.

$$MC\% = \frac{m_1 - m_2}{m_1} \cdot 100 \qquad (1)$$

The solubility of active films was assessed using a modified method based on Meerasri et al.[19] Samples (1×2 cm²) were dried at 105 °C for 24 hours to a constant weight, cooled, weighed (m'), and then immersed in 20 mL of distilled water for 24 hours. The remaining insoluble material was then dried at 105 °C for 24 hours, cooled, and reweighed (m'') to determine solubility.

$$TSM(\%) = \frac{m' - m''}{m'} \cdot 100 \qquad (2)$$

Water vapor transmission rate (WVTR) was determined according to ASTM E-996-00 (ASTM, 2000) with some modifications. The procedure involved the following steps: (1) 8 ml of distilled water was poured into each glass jar (mouth diameter: 3 cm, height: 5.3 cm) to create a relative humidity of 100%. (2) The mouth of each jar was then covered with a film (test sample). (3) The sealed jars were placed in a drying oven set at 40 °C. (4) The jars were weighed every 24 hours (accuracy 0.0001 g, measured at least 3 times) for a 24-hour period. (5) Linear regression was used to monitor the change in mass over time. The formula for water vapor transmission rate (WVTR (g.h⁻¹.m⁻²)) was calculated as follows:

$$WVTR = \frac{\Delta m}{A \times \Delta t} \qquad (3)$$

In which: Δm is mass loss of water in the glass jar (g); A is area of the film through which water vapor permeates ($= 7.06 \times 10^{-4}$ m²); Δt: time (hour).

2.3.2. Fourier Transform Infrared (FTIR) spectroscopy, Scanning Electron Microscopy (SEM), and evaluation of their thermal stability

FTIR spectroscopy was used to analyze the infrared spectra of the fabricated films. Measurements were taken from 400 to 4000 cm⁻¹ at a resolution of 4 cm⁻¹, averaging 32 scans

(Iffranity1s, Shimadzu, Japan). The surface and cross-sectional structures of the packaging films were examined using a scanning electron microscope (Hitachi S-4800, Japan) at an accelerating voltage of 5 kV. Before imaging, samples were coated with gold for 200 seconds using a sputter coater and mounted on aluminum stubs with conductive adhesive to improve conductivity. The thermal properties of the polymer films were studied using a Labsys Evo differential scanning calorimeter (France). Thermogravimetric analysis was performed under air flow (50 mL/min) at a temperature range from 25 to 600 °C at a heating rate of 10 °C/min.

2.3.3. Thickness and mechanical properties

Film thickness was measured with a digital micrometer (Mitutoyo Co., Tokyo, Japan) with a precision of ±0.001 mm. Each film sample underwent five measurements at randomly selected points. The mean thickness was calculated and used to determine additional parameters, such as mechanical properties and water vapor permeability. Tensile strength (TS) and elongation at break (EB) were evaluated according to the ASTM D882 standard (ASTM, 2002) using a Mark-10 testing machine (USA). Rectangular film specimens measuring 8×2 cm were prepared. The initial gap between clamps was set at 60 mm, and a 100 N load cell was used. TS was calculated as follows:

$$TS(MPa) = \frac{F_{max}}{\Phi} \qquad (4)$$

In which: Fmax: maximum measured force (N); Φ: cross-sectional area of the membrane (mm²).

The elongation at break is calculated by the following formula:

$$EB(\%) = \frac{\Delta l}{l_0} \times 100 \qquad (5)$$

Where: Δl is the measured elongation of the film sample during testing, expressed in millimeters (mm). l_0 is the initial length

of the sample prior to testing, expressed in millimeters (mm).

2.4. Antibacterial testing

To assess antibacterial properties, *Staphylococcus aureus* (PTCC 1112) and *Escherichia coli* (PTCC 1270) were chosen as representatives of Gram-positive and Gram-negative bacteria, respectively. The antibacterial performance was tested using the agar well diffusion method. Bacterial suspensions (0.1 mL, 10^7 CFU/mL) were evenly spread onto agar plates. Film samples were cut into 18 mm discs, consistent with commercial standards, and placed on the inoculated agar surfaces. The plates were then incubated at 37 °C for 24 hours. The effectiveness of the films was determined by measuring the diameter of the inhibition zones formed around each sample. The zone of inhibition (ZOI) was calculated using the formula:

$$ZOI \ (mm) = D - d \qquad (6)$$

In this equation, D refers to the diameter of the inhibition zone (in mm), while d represents the diameter of the agar well (in mm).

2.5. Antioxidant activity

A 2 mmol/L DPPH solution in 70% ethanol was prepared. 2 mL of this solution was added to stoppered vials containing 2 mg film samples. The vials were wrapped in aluminum foil and incubated for 30 minutes before measuring absorbance at 517 nm using a spectrophotometer (Shimadzu UV1800). All measurements were performed in triplicate. The percentage of DPPH free radical scavenging activity was then calculated.

$$\%DPPH = \frac{Abs_{DPPH} - Abs_{Sample}}{Abs_{DPPH}} \times 100 \qquad (7)$$

Where: Abs_{DPPH} is the absorbance of the blank DPPH solution at 517 nm; Abs_{sample} is the absorbance of the film-treated sample at the same wavelength.

3. RESULTS AND DISCUSSION

3.1. Characterization of CA/SA/OEO active films

3.1.1. Chemical structures analysis

Figure 1 shows the FT-IR spectra of the prepared films. The spectra exhibited characteristic peaks of cellulose acetate (~1735 cm⁻¹ for C=O ester, ~1215 cm⁻¹ for C–O ester, and ~1029 cm⁻¹ for C–O–C).[7] The band at 3498 cm⁻¹, representing free OH groups in the CA polymer, was significantly reduced in the films incorporating OEO emulsion. This reduction indicates that embedding OEOs into the CA matrix limits the presence of free OH groups, thereby improving the water barrier properties of the film. The peaks at approximately 1637 and 1410 cm⁻¹ correspond to the COO⁻ vibration of COO⁻ symmetric stretch of alginate. The increased intensity at 2949 cm⁻¹ (C–H stretching)[14] indicated the presence of OEO in the film matrix. The absorption peak at around 1561 cm⁻¹ transformed into a series of small peaks in the range of 1500–1600 cm⁻¹, and peaks at 1508 cm⁻¹ (conjugated groups) and 1457 cm⁻¹ (-CH₂ bending vibration) confirmed the effective incorporation of OEO into the films.[20] The peaks at 810 cm⁻¹ (C–H bending), 939 cm⁻¹ (C–C bending vibration), and 1178 cm⁻¹ (C-O-C stretching) were either very weak or not observed. The observed peak shifts imply molecular interactions among CA, SA, and OEO components during their dispersion within the film matrix.[21]
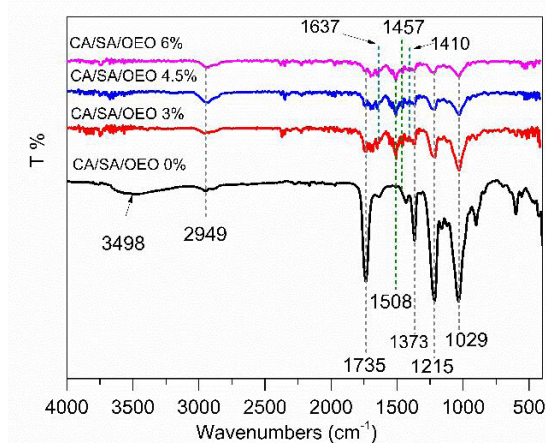

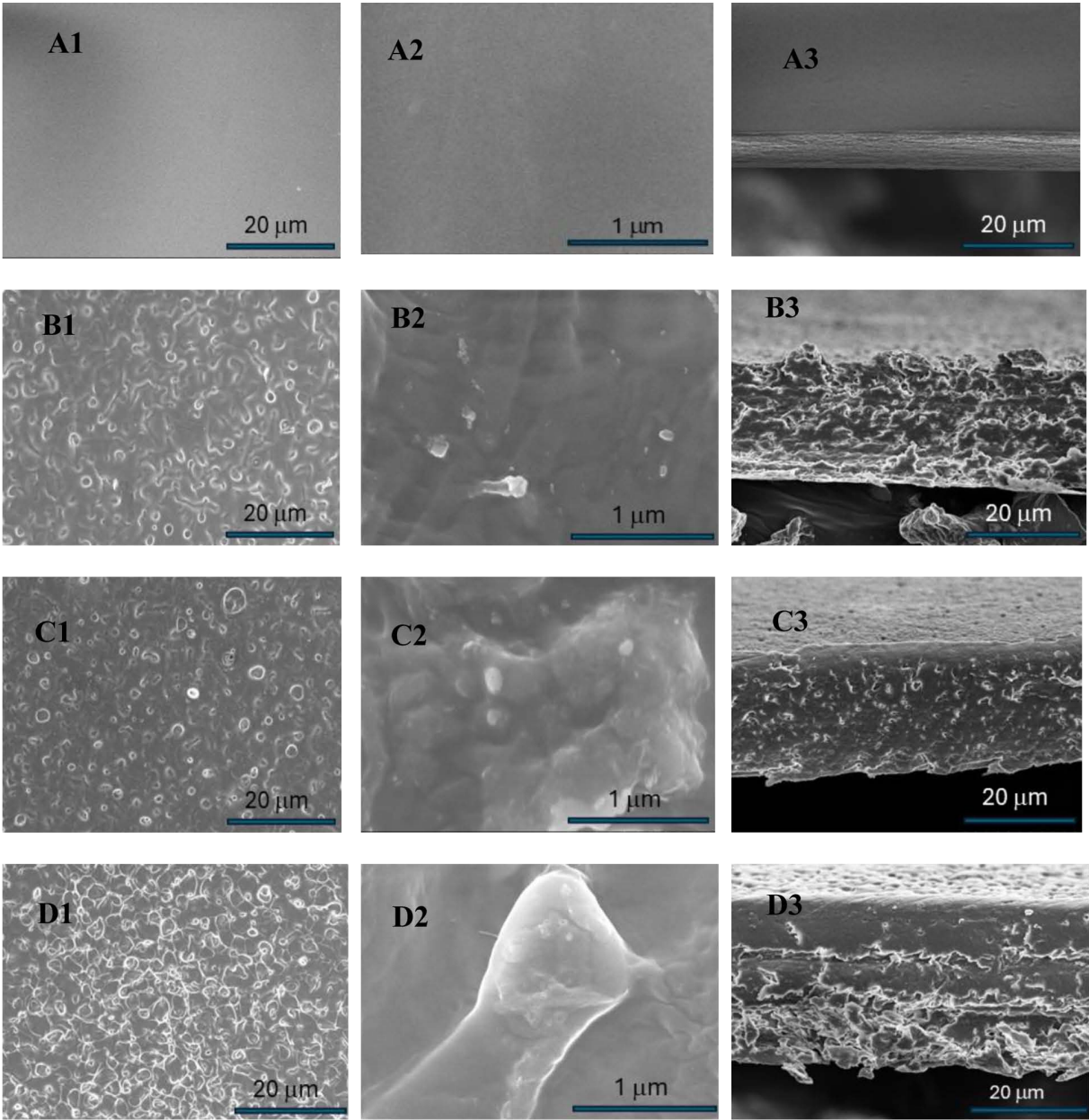**Figure 1.** FTIR spectra of CA/SA/OEO films.

Figure 2. SEM images of surface (1, 2) and cross-section (3) of active films: (A1, A2, A3) CA/SA/OEO 0%; (B1, B2, B3) CA/SA/OEO 3%; (C1, C2, C3) CA/SA/OEO 4.5%; (D1, D2, D3) CA/SA/OEO 6%.

Table 1. Moisture content (MC), total soluble matter (TSM), water vapor transmission rate (WVTR), thickness, tensile strength (TS) and elongation at break (EB) of the CA/SA/OEO films.

Films	MC (%)	TSM (%)	WVTR $(g.h^{-1}.m^{-2})$	Thickness (mm)	TS (MPa)	EB (%)
CA/SA/OEO 0%	8.32 ± 0.21	0.01 ± 0.01	46.86 ± 0.33	0.007 ± 0.003	33.32 ± 0.12	4.60 ± 0.92
CA/SA/OEO 3%	4.92 ± 0.06	2.50 ± 0.12	15.13 ± 0.14	0.021 ± 0.001	31.42 ± 1.59	4.88 ± 0.94
CA/SA/OEO 4.5%	1.35 ± 0.14	1.51 ± 0.05	8.58 ± 0.29	0.023 ± 0.005	16.76 ± 0.30	18.03 ± 3.28
CA/SA/OEO 6%	1.26 ± 0.02	2.36 ± 0.23	10.26 ± 0.52	0.032 ± 0.002	15.52 ± 1.22	4.82 ± 0.372

3.2.2. Morphologies analysis

Figure 2 presents SEM images illustrating the surface and cross-sectional morphology of CA and OEO emulsion incorporated films. SEM analysis revealed that the surface and cross-sectional views of the CA/SA/OEO 0% film were smooth and intact, with no visible holes or cracks, which was uniformly distributed and well-dispersed, without significant agglomerations (Figure 2.A1, 2.A2, 2.A3). Films containing 3, 4.5, and 6% OEO emulsion exhibit increased surface roughness characterized by valley-like grooves and circular bumps (Figure 2.B1, 2.C1, 2.D1). This surface morphology suggests effective encapsulation of OEO within the film, as indicated by the presence of sodium alginate (SA), Tween 80, and OEO from the emulsion. Emulsion instability during the drying process results in surface irregularities.[22] At higher magnifications (Figure 2.A2, 2.B2, 2.C2, 2.D2), SEM images illustrate the dispersion of OEO particles within the CA matrix. In the CA/SA/OEO 4.5% film, the microparticles appear well-distributed and stable. However, in the film containing 6% OEO, particle agglomeration becomes evident, contributing to a noticeably rougher surface compared to the other OEO-containing films. Analysis of cross-sectional SEM images (Figure 2.A3, 2.B3, 2.C3, 2.D3) demonstrates that film thickness increases as the concentration of OEO emulsion rises, consistent with the thickness measurements in Table 1. The observation of cross-sectional pores (Figure 2.B3, 2.C3, 2.D3) further confirms the embedding of OEO within the film matrix, which aligns with findings reported by Xu et al.[23] The incorporation of OEO particles expands the spacing between CA chains, leading to an increase in the thickness of films. The film containing 4.5% OEO exhibits uniformly distributed particles and pores within the CA matrix.

3.2.3. Thermal stability analysis

Figure 3 illustrates the thermal degradation of the films via TGA and dTG analyses. The thermal degradation of pure CA (CA/SA/OEO 0%, Figure 3.A) occurs in three distinct stages. The first stage, observed up to 120 °C, corresponds to a mass loss of 9.7%, primarily due to the evaporation of moisture and residual solvents.[24]
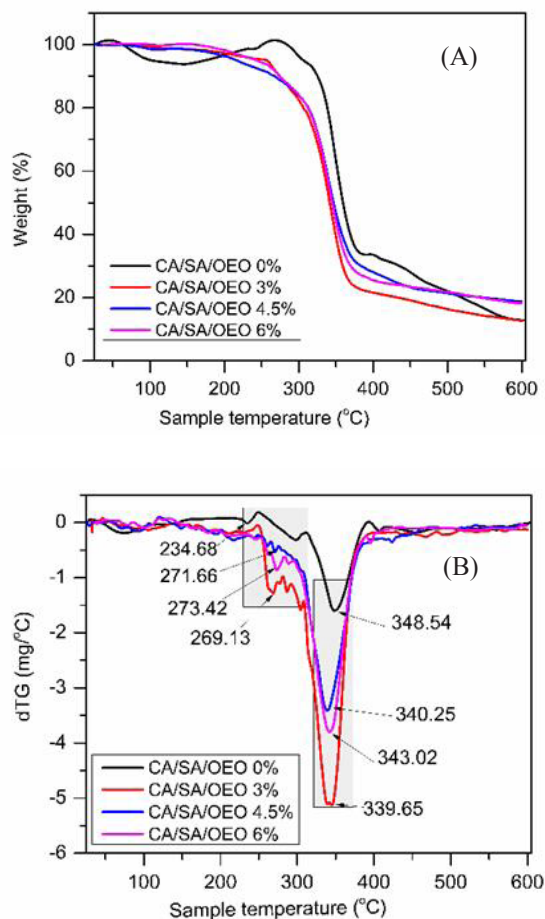

Figure 3. TG curves (A) and DTG curves (B) of fabricated films.

This mass loss was greater than that observed in the films containing OEO, indicating a higher moisture content, which aligns with the moisture values presented in Table 1. The second stage, occurring between 250 °C and 400 °C, is identified as the main thermal decomposition phase, with a significant mass loss of 90.04%. This stage is attributed to the breakdown of the CA polymer backbone, cleavage of glycosidic linkages, and the formation of furanic compounds.[10] The third stage, above 500 °C, represents the final degradation phase, associated with complete decomposition and

carbonization of the sample. Similar to pure CA, the OEO-containing films also exhibited three distinct degradation stages. However, during the main decomposition stage, two separate mass loss events were observed, corresponding to the thermal degradation of sodium alginate (SA) between 250 °C and 280 °C.[24,18] Notably, the mass loss for the CA/SA/OEO 4.5% film in this stage was 5.98% lower than that of the CA/SA/OEO 6% (12.39%) and CA/SA/OEO 3% (20.49%) films. The third stage occurs between 300 °C and 400 °C. At this stage, the mass loss for the CA/SA/OEO 4.5% film was approximately 75.26% higher than that of the CA/SA/OEO 3% film, which had a mass loss of about 66.93%, and the CA/SA/OEO 6% film, which had a mass loss of 69.54%. The primary cause of quality deterioration in this stage is the breakdown of the deacetylation of CA. The total mass loss in stage 2 of the CA/SA/OEO 4.5% film is 81.24%, exhibiting significantly lower mass loss compared to the films containing 3% and 6% OEO. The CA/SA/OEO 4.5% film demonstrated higher residual mass and improved thermodynamic stability when exposed to temperatures exceeding 550 °C. The dTG, which represents the first-order derivative of TGA, is shown in Figure 3B. The peak temperature in the dTG curve, indicating the highest degradation rate, is defined as the maximum degradation temperature (T_m). A slight decrease in T_m was observed with increasing OEO content, suggesting a minor reduction in thermal stability. This behavior may result from interactions among CA, OEO, and SA, which also influence the overall mass loss of the films.

3.2. Analysis of moisture content, total soluble matter and water vapor transmission rate

As shown in Table 1, the moisture content decreased with increasing OEO emulsion amount in the films. The moisture content ranges from 8.32% for CA/SA/OEO 0% film to 1.26% for CA/SA/OEO 6% film. The incorporation of OEO contributes to the hydrophobic nature of the film surface.[19] Additionally, cross-linking between the CA polymer and OEO may further

reduce moisture content.[25] A study by Jiang et al. found that adding essential oil to multilayer gelatin/myofibrillar films decreased their wettability.[26]

Film solubility, expressed as total soluble matter (TSM), is a critical parameter for packaging moisture-rich foods such as fruits. Lower solubility enhances structural integrity in humid environments, contributing to extended shelf life and reduced nutrient, water, and flavor loss.[27] Among the tested films, CA/SA/OEO 4.5% exhibited the lowest solubility (1.51%), making it the most suitable for humid conditions. In contrast, the higher solubility of CA/SA/OEO 3% may compromise its preservation performance. The interaction between OEO emulsion and the film matrix disrupted intermolecular forces and formed bonds with hydroxyl groups.[10] This interaction reduced the film's solubility in water.

Water Vapor Transmission Rate (WVTR) is a critical parameter in food packaging, as moisture plays a key role in maintaining product stability and controlling microbial growth-both essential for preserving food quality. Films with high WVTR allow moisture to escape, potentially leading to dehydration and quality degradation. Conversely, low WVTR may cause moisture accumulation, promoting bacterial and mold growth. For specific packaging applications, increasing film thickness or using high-barrier materials typically achieves the required gas transmission rates. Incorporating hydrophobic OEO emulsion droplets into the CA matrix increased both hydrophobicity and the complexity of the water vapor diffusion pathway. Intermolecular interactions between the OEO emulsion and CA chains resulted in a denser surface structure. Of the samples tested, the CA/SA/OEO 4,5% film demonstrated the best water vapor barrier properties, likely due to its uniform structure as shown in SEM images (Figure 2). In comparison, 3% and 6% films showed uneven emulsion droplet distribution, which disrupted the compact CA structure and created pores and internal cavities that increased water vapor diffusion. While the pristine CA film was tightly

packed, its thinner and more hydrophilic nature led to a higher WVTR value.

3.3. Mechanical properties of CA/SA/OEO active films

3.3.1. The thickness

Table 1 shows that the addition of OEO emulsion significantly increased film thickness compared to the CA film. This finding is consistent with previous research indicating that plasticizers and lipid-based substances increase film thickness. Employing an optimal surfactant-to-oil ratio and sufficient acoustic energy during emulsification improved the stability of the film-forming solution during drying. This approach reduced OEO emulsion loss and increased film thickness.[27] The generation of microdroplets from hydrophobic OEO during homogenization also contributed to this outcome. Furthermore, higher concentrations of OEO emulsion increased the total solid content in the solution, further enhancing the final film thickness.

3.3.2. Tensile strength and elongation at break

Tensile strength (TS) and elongation are crucial factors for food packaging films. Films with high tensile strength are less likely to tear under stress, making them suitable for applications that require significant mechanical strength. In contrast, films with high elongation can stretch well and are less likely to break when bent or stretched, which is particularly important in stretch packaging or in applications that demand flexibility.[28] Table 1 demonstrates that incorporating OEO produced a typical plasticizing effect, marked by a decline in TS and an increase in elongation at break (EB).[7] Pure CA film's rigidity and brittleness are reflected in its high TS (33.32 MPa) and EB of 4.60%. The incorporation of OEO emulsion into CA films resulted in a decrease in TS and a notable increase in EB. This mechanical behavior is attributed to molecular-level interactions between OEO emulsion and CA chains. Specifically, the well-dispersed OEO emulsion disrupts the intermolecular hydrogen bonding among CA chains,[10] leading to an increase in free volume and enhanced polymer chain flexibility.[29] The hydrophobic constituents of OEO, such as carvacrol and thymol, interact with the CA matrix primarily through van der Waals forces, which are weaker than hydrogen bonds. These interactions are evidenced by the reduced intensity of the O–H stretching band in the FTIR spectrum (Figure 1), indicating a weakening of hydrogen bonding. Additionally, shifts or decreases in the C=O and C–O stretching bands (Figure 1) suggest increased free volume and reduced intermolecular cohesion, consistent with the plasticizing effect of OEO.[2] However, when OEO is added in excess, it can form dispersed droplets within the film matrix (Figure 2.D2), which act as localized stress points. These microstructural discontinuities can slightly reduce EB due to uneven stress distribution during deformation. Consequently, the optimal CA/SA/OEO and Tween 80 ratios in the CA/SA/OEO 4.5% film demonstrate good compatibility, significantly improving elongation. According to Alqahtani et al., biodegradable films with tensile strengths ranging from 1 to 10 MPa are deemed acceptable for practical use.[28] Since all the prepared films have tensile strengths above 10 MPa, they are suitable for practical applications in active packaging.

3.4. Antibacterial and antioxidant properties

Figure 4 presents the antibacterial activity test results for as-prepared active films. Initially, the CA film without OEO did not show antibacterial inhibition zones, but no bacteria appeared on the film surface. In contrast, the OEO films demonstrated a distinct antibacterial zone. The determined by the concentration of carvacrol, its most active compound, as well as other phenolic constituents such as thymol and p-cymene, which act synergistically. These compounds disrupt bacterial outer membranes, increase permeability, and result in the loss of ions, adenosine triphosphate (ATP), and other cytoplasmic components, thereby inhibiting bacterial growth.[30] Subsequently, Table 2 displays the inhibition zone (ZOI) values for films tested against *E.Coli* and *S.aureus*. Analysis of these results shows that membrane CA/SA/OEO

4.5% exhibits the highest antibacterial activity, followed by CA/SA/OEO 6%. Overall, these findings suggest that the OEO emulsion with sodium alginate (SA) and Tween 80 effectively stabilizes OEO in microparticle form within the film matrix, which minimizes loss during film formation.

The antioxidant activity of the films was evaluated using various concentrations of film extract solutions (Table 3). According to the DPPH assay, the CA/SA/OEO 6% film exhibited the highest radical scavenging activity, reaching 84.2% after 12 hours. As expected, the pristine CA film showed no antioxidant activity due to the absence of active compounds. The observed increase in antioxidant performance results from bioactive compounds present in oregano essential oil, including thymol and carvacrol. These compounds donate electrons or hydrogen atoms to neutralize free radicals. The DPPH% values presented in Table 3 demonstrate a consistent increase in antioxidant activity over time, suggesting a gradual and sustained release of essential oil from the film matrix. However, at higher concentrations, the essential oil may aggregate or distribute unevenly, potentially compromising the mechanical integrity and altering the surface morphology of the films.
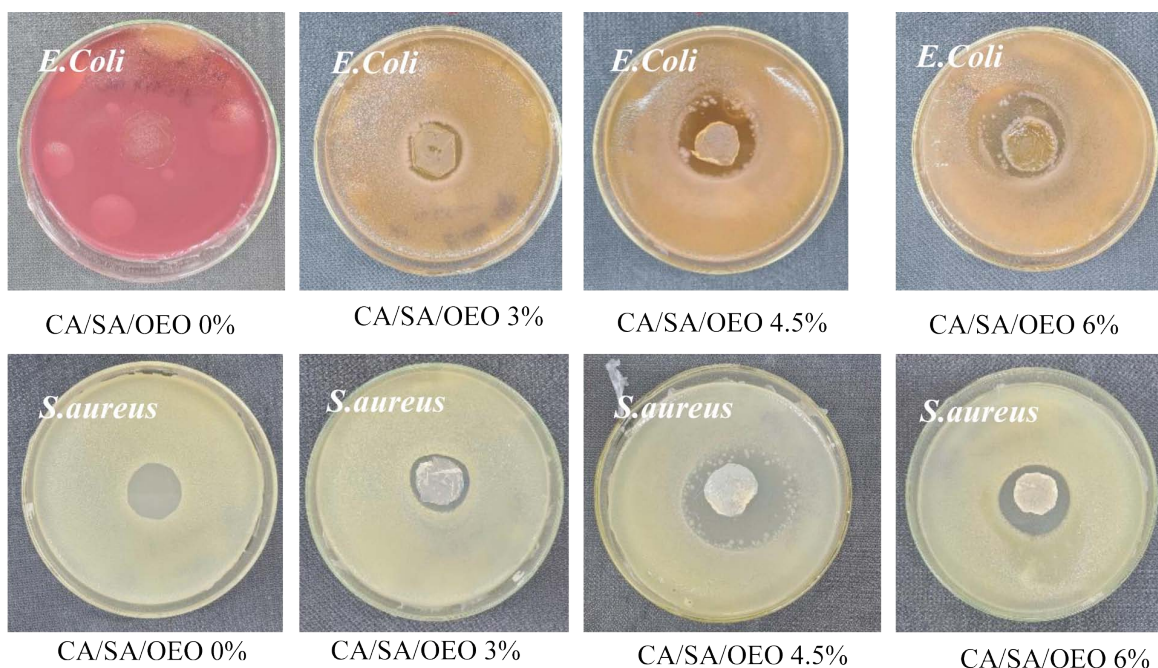

Figure 4. Photographs of inhibition zones formed by active films against *E. Coli* and *S.aureus*.

Table 2. Zone of inhibition (ZOI) values of the films against *E. Coli* and *S.aureus*.

Films	ZOI (*E. Coli*) (mm)	ZOI (*S.aureus*) (mm)
CA/SA/OEO 0%	nd	nd
CA/SA/OEO 3%	25 ± 0.3	25 ± 0.2
CA/SA/OEO 4.5%	35 ± 0.1	44 ± 0.1
CA/SA/OEO 6%	34 ± 0.1	33 ± 0.3

Table 3. DPPH Radical Scavenging Activity of CA/SA/OEO films.

Films	DPPH (%) 30 min	DPPH (%) 60 min	DPPH (%) 12 hour
CA/SA/OEO 0%	0	0	0
CA/SA/OEO 3%	36.3 ± 0.2	69.3 ± 0.1	83.2 ± 0.3
CA/SA/OEO 4.5%	39.9 ± 0.2	75.5 0.3	84.0 ± 0.1
CA/SA/OEO 6%	45.8 ± 0.1	79.6 ± 0.5	84.2 ± 0.4

4. CONCLUSION

This study highlights the potential of cellulose acetate films with oregano essential oil emulsion, prepared using sodium alginate and Tween 80, as active packaging materials with improved antibacterial, antioxidant, and water barrier properties. The CA/SA/OEO 4.5% formulation achieved 84% DPPH radical scavenging activity, indicating sustained essential oil release. Antimicrobial tests showed inhibition zones of 35 mm for *E. Coli* and 44 mm for *S. aureus*, confirming strong antibacterial effects. SEM analysis showed that uniform emulsion droplet dispersion enhanced film morphology and barrier performance, while higher OEO concentrations led to aggregation and structural irregularities. These findings support the use of ternary CA composites as active packaging to extend the shelf life of various food products.

REFERENCES

1. F. Pavli, A. A. Argyri, P. Skandamis, G. J. Nychas, C. Tassou, N. Chorianopoulos. Antimicrobial activity of oregano essential oil incorporated in sodium alginate edible films: control of listeria monocytogenes and spoilage in ham slices treated with high pressure processing, *Materials (Basel)*, **2019**, *12*(22), 3726.

2. F. G. Fernandes, C. V. B. Grisi, R. d. C. Araújo, D. A. Botrel, S. d. Sousa. Active cellulose acetate-oregano essential oil films to conservation of hamburger buns: antifungal, analysed sensorial and mechanical properties, *Packaging Technology and Science* **2022**, *35*(2), 175-182.

3. H. Falleh, M. Ben Jemaa, M. Saada, R. Ksouri. Essential oils: a promising eco-friendly food preservative, *Food Chemistry,* **2020**, *330*, 127268.

4. F. Han, G. Q. Ma, M. Yang, L. Yan, W. Xiong, J. C. Shu, Z. D. Zhao, H. L. Xu. Chemical composition and antioxidant activities of essential oils from different parts of the oregano, *Journal of Zhejiang University Science B,* **2017**, *18*(1), 79-84.

5. B. Malhotra, A. Keshwani, H. Kharkwal. Antimicrobial food packaging: potential and pitfalls, *Frontiers in Microbiology,* **2015**, *6*, 611.

6. B. Tian, J. Liu, W. Yang, J. B. Wan. Biopolymer food packaging films incorporated with essential oils, *Journal of Agricultural and Food Chemistry,* **2023**, *71*(3), 1325-1347.

7. C. C. Pola, E. A. A. Medeiros, O. L. Pereira, V. G. L. Souza, C. G. Otoni, G. P. Camilloto, N. F. F. Soares. Cellulose acetate active films incorporated with oregano (Origanum vulgare) essential oil and organophilic montmorillonite clay control the growth of phytopathogenic fungi, *Food Packaging and Shelf Life,* **2016**, *9*, 69-78.

8. D. A. Laroque, G. M. F. Aragão, P. H. H. Araújo, B. A. M. Carciofi. Active cellulose acetate-carvacrol films: antibacterial, physical and thermal properties, *Packaging Technology and Science,* **2021**, *34*, (8), 463-474.

9. N. Dairi, H. F. Harrar, M. Ramos, M. C. Garrigos. Cellulose acetate/AgNPs-organoclay and/or thymol nano-biocomposite films with combined antimicrobial/antioxidant properties for active food packaging use, *International Journal of Biological Macromolecules,* **2019**, *121*, 508-523.

10. T. Erceg, N. Vukić, O. Šovljanski, A. Stupar, V. Šergelj, M. Aćimović, S. Baloš, J. Ugarković, D. Šuput, S. Popović, S. a. Rakić. Characterization of films based on cellulose acetate/poly(caprolactone diol) intended for active packaging prepared by green chemistry principles, *ACS Sustainable Chemistry & Engineering,* **2022**, *10*(28), 9141-9154.

11. Y. Zeng, Y. Wang, J. Tang, H. Zhang, J. Dai, S. Li, J. Yan, W. Qin, Y. Liu. Preparation of sodium alginate/konjac glucomannan active films containing lycopene microcapsules and the effects of these films on sweet cherry

preservation, *International Journal of Biological Macromolecules,* **2022**, *215*, 67-78.

12. F. N. Nkede, A. A. Wardana, N. T. H. Phuong, Y. Xirui, A. Koga, M. H. Wardak, F. Tanaka, F. Tanaka. Improved alginate-based films by Ylang-ylang (Cananga odorata L) oil incorporation, *Polymers for Advanced Technologies,* **2023**, *34*(7), 2213-2223.

13. R. He, W. Chen, Q. Zhong, M. Zhang, J. Pei, W. Chen, H. Chen. Sodium alginate emulsion loaded with linalool: preparation, characterization and antibacterial mechanism against Shigella sonnei, *International Journal of Biological Macromolecules,* **2023**, *244*, 125167.

14. C. Wang, Z. Song, Y. Cao, L. Han, Q. Yu, G. Han, X. Zhu. Characterization of sodium alginate-carrageenan films prepared by adding peanut shell flavonoids as an antioxidant: application in chilled pork preservation, *International Journal of Biological Macromolecules,* **2024**, *266*(1), 131081.

15. P. Yan, W. Lan, J. Xie. Modification on sodium alginate for food preservation: a review, *Trends in Food Science & Technology,* **2024**, *143*, 104217.

16. H. Saffarian, E. Rahimi, F. Khamesipour, S. M. H. Dehkordi. Antioxidant and antimicrobial effect of sodium alginate nanoemulsion coating enriched with oregano essential oil (Origanum vulgare L.) and Trachyspermum ammi oil (Carum cupticum) on food pathogenic bacteria, *Food Science and Nutrition,* **2024**, *12*(4), 2985-2997.

17. J. Baranauskaite, M. A. Ockun, B. Uner, C. Tas, L. Ivanauskas. Effect of the amount of polysorbate 80 and oregano essential oil on the emulsion stability and characterization properties of sodium alginate microcapsules, *Molecules,* **2021**, *26*(20), 6304.

18. X. Tian, X. Huo, X. Li, D. Wang, J. Lu, X. Ren, Q. Kong. Characterization of the sodium alginate/ essential oil emulsion film and its efficacy in controlling postharvest Penicillium expansum disease in cherry tomatoes, *International Journal of Biological Macromolecules,* **2025**, *318*(1), 144853.

19. J. Meerasri, U. Sukatta, P. Rugthaworn, K. Klinsukhon, L. Khacharat, S. Sakayaroj, R. Chollakup, R. Sothornvit. Synergistic effects of thyme and oregano essential oil combinations for enhanced functional properties of sericin/ pectin film, *International Journal of Biological Macromolecules,* **2024**, *263*(1), 130288.

20. K. Wang, Y. Wang, M. Cheng, Y. Wang, P. Zhao, X. Xi, J. Lu, X. Wang, X. Han, J. Wang. Preparation and characterization of active films based on oregano essential oil microcapsules/ soybean protein isolate/sodium carboxymethyl cellulose, *International Journal of Biological Macromolecules,* **2024**, *258*(2), 128985.

21. K. Munhuweyi, O. J. Caleb, A. J. v. Reenen, U. L. Opara. Physical and antifungal properties of β-cyclodextrin microcapsules and nanofibre films containing cinnamon and oregano essential oils, *LWT,* **2018**, *87*, 413-422.

22. M. Xiao, L. Luo, B. Tang, J. Qin, K. Wu, F. Jiang. Physical, structural, and water barrier properties of emulsified blend film based on konjac glucomannan/agar/gum Arabic incorporating virgin coconut oil, *LWT,* **2022**, *154*, 112683.

23. J. Xu, M. He, C. Wei, M. Duan, S. Yu, D. Li, W. Zhong, C. Tong, J. Pang, C. J. F. H. Wu. Konjac glucomannan films with Pickering emulsion stabilized by TEMPO-oxidized chitin nanocrystal for active food packaging, *Food Hydrocolloids,* **2023**, *139*, 108539.

24. H. Wang, M. Li, R. Ren, Z. Gao, L. Meng, Z. Li, C. Cao. Preparation of sodium alginate antibacterial porous composite pads embedded with centrifugally spun nanofibers by freeze-drying and recasting for active food packaging, *Carbohydrate Polymers,* **2025**, *355*, 123430.

25. B. Ocak. Properties and characterization of thyme essential oil incorporated collagen hydrolysate films extracted from hide fleshing wastes for active packaging, *Environmental Science and Pollution Research,* **2020**, *27*(23), 29019-29030.

26. J. Jiang, P. S. M. S. L. Watowita, R. Chen, Y. Shi, K. T. J. T. Geng, L. Li, K. Osako. Multilayer gelatin/myofibrillar films containing clove essential oil: properties, protein phenolic

interactions, and migration of active compounds, *Food Packaging and Shelf Life,* **2022**, *32*, 100842.

27. H. Yu, C. Zhang, Y. Xie, J. Mei, J. Xie. Effect of melissa officinalis L. essential oil nanoemulsions on structure and properties of Carboxymethyl chitosan/locust bean gum composite films, *Membranes (Basel),* **2022**, *12*(6), 568.

28. N. Alqahtani, T. Alnemr, S. Ali. Development of low-cost biodegradable films from corn starch and date palm pits (Phoenix dactylifera), *Food Bioscience,* **2021**, *42*, 101199.

29. Y. Zhao, H. Sun, B. Yang, Y. Weng. Hemicellulose-based film: potential green films for food packaging, *Polymers (Basel),* **2020**, *12*(8), 1775.

30. A. Sajimon, A. S. Edakkadan, A. J. Subhash, M. Ramya. Incorporating oregano (Origanum vulgare L.) essential oil onto whey protein concentrate based edible film towards sustainable active packaging, *Journal of Food Science and Technology,* **2023**, *60*(9), 2408-2422.